



Minnesota State University, Mankato
Cornerstone: A Collection of Scholarly
and Creative Works for Minnesota
State University, Mankato

All Graduate Theses, Dissertations, and Other
Capstone Projects


Graduate Theses, Dissertations, and Other
Capstone Projects

2012

Investigation into the Usability of Micromechanical Models to Predict the Behavior of a Nanocomposite Polymer

Jason Handlogten
Minnesota State University - Mankato

Follow this and additional works at: <https://cornerstone.lib.mnsu.edu/etds>

 Part of the [Industrial Engineering Commons](#), [Manufacturing Commons](#), and the [Materials Science and Engineering Commons](#)

Recommended Citation

Handlogten, J. (2012). Investigation into the Usability of Micromechanical Models to Predict the Behavior of a Nanocomposite Polymer [Master's thesis, Minnesota State University, Mankato]. Cornerstone: A Collection of Scholarly and Creative Works for Minnesota State University, Mankato. <https://cornerstone.lib.mnsu.edu/etds/176/>

This Thesis is brought to you for free and open access by the Graduate Theses, Dissertations, and Other Capstone Projects at Cornerstone: A Collection of Scholarly and Creative Works for Minnesota State University, Mankato. It has been accepted for inclusion in All Graduate Theses, Dissertations, and Other Capstone Projects by an authorized administrator of Cornerstone: A Collection of Scholarly and Creative Works for Minnesota State University, Mankato.

Investigation into the Usability of Micromechanical Models to
Predict the Behavior of a Nanocomposite Polymer

By

Jason Handlogten

A Thesis Submitted in Partial Fulfillment of the

Requirements for the Degree of

Master of Science

In

Manufacturing Engineering Technology

Minnesota State University, Mankato

Mankato, Minnesota

May of 2012

Investigation into the Usability of Micromechanical Models to Predict the Behavior of a Nanocomposite Polymer

Jason Handlogten

This thesis has been examined and approved by the following members of the thesis committee.

Dr. William Peterson, Advisor

Dr. Guanghsu Chang

Dr. Harry Petersen

Table of Contents

Chapter 1: Introduction	1
Chapter 2: Literature Review	7
Equation 1 – Young’s Modulus.....	15
Table 1 – Young’s and Shear Modulus Results from Models.....	16
Table 2 – Mechanical Properties of Components of a Sample Composite.....	17
Chapter 3: Methodology	18
Chapter 4: Findings from Tensile Testing	25
Figure 1 – First Four Specimens after Tensile Test.....	26
Chapter 5: Revised Methodology and Results	27
Figure 2 – All Five Specimens after Tensile Test.....	27
Figure 3 – Specimens that were Tested Twice.....	28
Figure 4 – Specimens with Ends Cut Off.....	29
Figure 5 – Specimen after Impact Test.....	30
Figure 6 – Specimen that was cut into Slices.....	30
Figure 7 – Specimen with end cut at Diagonal.....	31
Figure 8 – Partial Core Exposed after Attempting Diagonal Cut.....	32
Chapter 6: Conclusion and Future Research	33
Figure 9 – All Stress Strain Curve of a Test Specimen after Tensile Test.....	33
Reference List	37
Appendix A: CMM Code and Data Collection for a Test Specimen	39
Appendix B: Young’s and Shear Modulus Predictions by Models	50

Abstract

This thesis, “Investigation into the Usability of Micromechanical Models to Predict the Behavior of a Nanocomposite Polymer”, was written by Jason Handlogten as part of a Master of Science of Manufacturing Engineering Technology from Minnesota State University – Mankato in 2012.

The purpose of this thesis was to determine the acceptability of a set of existing nanocomposite test specimens for tensile testing and then to determine the Young’s and shear modulus of these test specimens. If the test specimens were found to be acceptable, the accuracy of three micromechanical models was to be evaluated by comparing their predictions to the mechanical properties determined from testing the specimens.

The set of existing nanocomposite test specimens had a distinct concave shape on two surfaces that were believed to be intended as flat. In order to determine if they adhered to the Type I geometry for reinforced composites as listed in the *Standard Test Method for Tensile Properties of Plastics* a program was written using a coordinate measuring machine to measure the cross sectional area of the test specimens. The geometry was found to meet the requirements of the standard and then the tensile testing procedure from the standard was followed.

During process verification of the testing procedure, the specimens were found to behave in an unexpected way for a material that was supposed to be homogeneous and isotropic. The test specimens were found to consistently break outside of the narrow test section.

An investigation into the behavior of the test specimens using dissection, impact testing, and hardness testing found that a core had formed inside the test specimens during fabrication and therefore the specimens were not homogeneous and isotropic.

Since the three micromechanical models under investigation for this thesis had the assumption that the material is homogeneous and isotropic it was determined that the three micromechanical models should not be used to predict the mechanical properties of the set of test specimens.

Chapter 1 – Introduction

Micromechanical analytical models are an important tool used by engineers to estimate mechanical properties during preliminary design stages as well as during manufacturing (Park, 2007). Use of analytical models is especially important when dealing with composite materials. One of the primary benefits of using composite materials is that the specific properties of the composite can be adjusted by varying the geometry and concentration of the reinforcement; this allows for near custom properties for specific applications.

Composite polymers generally consist of two phases. The continuous phase is known as the matrix. This is usually the polymer that is going to be reinforced. The discontinuous phase is known as the reinforcement. This is the material added to the polymer in an attempt to improve the properties of the composite (Agarwal, 1990). Various types of reinforcements can be used with polymers to enhance certain mechanical properties of the polymer. It is important to take into account the geometry of the reinforcement being used because shape, size, and distribution will alter the properties of the composite (Agarwal, 1990). Traditional composite polymers use fibers, short fibers, or platelets as reinforcements. Although the reinforcement of polymers using fillers is common in modern plastics, polymer nanocomposites represent an alternative option to traditional filled polymers (Koo, 2006).

Recently, nano-size particles have been used to reinforce polymers; the first organo-clay hybrid nanocomposite was patented in 1976. The use of nano-size particles in composite polymers offers the potential for many improvements to material properties

such as changes in electrical resistance, flame retardation, as well as improvements in mechanical strength (Koo, 2006). Although there are potential benefits from using nano-size particles, there are also new challenges related to designing with and fabricating these new composites. Although there are several analytical models that attempt to predict the macromechanical properties of composite polymers, few models have been developed that attempt to take into account the consideration of filler and void content (Park, 2005).

Although the mechanical properties of a polymer can be determined by physical testing of the material, this requires that the specific composite has already been fabricated. Repeating the fabrication and testing processes is usually a time consuming and costly method to create a specific composite (Park, 2005). Significant time and cost savings can be taken advantage of if the composite material is designed concurrently with the application structure design. In order to properly use concurrent design of the nanocomposite, accurate mechanical models are necessary (Barbero, 2011).

Due to their small size, nanoparticles exhibit a significantly large surface area-to-volume ratio. By increasing the surface area-to-volume ratio of the reinforcement, a larger interfacial area is established. When the nanoparticles are well dispersed in the polymer, the immense interfacial area and the nanoscopic dimensions between the nanoparticles creates a fundamental difference between nanocomposites and traditional reinforced polymers; this fundamental difference implies that the properties of a nanocomposite cannot be predicted by simply scaling down models that are accurate for traditional polymers (Koo, 2006). The inability to simply scale down current models is

also hindered because it appears that materials tend to behave differently on the nano scale (Wilson, 2002).

An important material property often used during a design process to evaluate the strength of a material is the modulus of elasticity, also known as the Young's modulus. The Young's modulus is a ratio of the tensile stress and the tensile strain a material experiences during an axial load. In order to accurately determine the modulus of elasticity of a material, the stress and strain during the test need to be accurately obtained. Since the engineering stress a material experiences is calculated as a ratio of force over the original cross sectional area, the value used for the cross sectional area during calculations has a direct influence on the calculated modulus of elasticity (Schaffer, 1999).

The purpose of this thesis was to determine the acceptability of a set of existing nanocomposite test specimens for tensile testing and then to determine the Young's and shear modulus of these test specimens. If the test specimens were found to be acceptable, the accuracy of three micromechanical models was to be evaluated by comparing their predictions to the mechanical properties determined from testing the specimens.

Deliverables for this thesis were to include a procedure to measure the cross sectional area of the test specimens. Since the cross sectional area of the specimen has a direct relation to the calculated value for the mechanical properties, it is important that the cross section area be measured accurately. Due to the shrinkage of the material during the fabrication process, the existing set of specimens had a distinct concave shape along two surfaces which were believed to be intended as flat. Because of limitations in measuring equipment, determining the exact cross sectional area is not feasible, so a procedure was

to be developed to measure the cross sectional area to a degree of accuracy that would allow reasonable determination of the needed physical properties of the existing set of test specimens. This process would allow a single injection molding die to be used for a wide variety of materials. Even though each unique composition of materials would have a unique shrinkage rate, this process would allow the cross sectional area of any test specimen to be measured. This would prevent the need to create new or modify old injection molding dies each time a new material with an unknown shrinkage rate was to be studied.

The second deliverable for this thesis was to be an evaluation of the geometry of the existing set of test specimens to determine if they adhere to the ASTM D 638 standard; *Standard Test Method for Tensile Properties of Plastics*. The geometry of the existing test specimens were to be compared to the Type I specimen for reinforced composites as called out in the ASTM.

The third deliverable for this thesis will be to define the Young's and shear modulus of the nanocomposite test specimens based on the results of mechanical testing of the actual specimens.

If the test specimens were found to fail the geometrical requirements listed in ASTM D 638, a recommendation was to be made for a reasonable use of the existing test specimens. Even if the geometry was not able to meet the ASTM standards, a tensile test was still to be conducted so that preliminary research data would be collected. Additionally, a recommendation was to be made as to what should be done with the die that was used to create the test specimens. The recommendation was to provide guidelines so that test specimens that conform to the required geometry could be made.

The fourth deliverable for this thesis will be a determination of selected characteristics of the set of test specimens. The characteristics that will be examined are the Young's and shear modulus. The Young's and shear modulus of each test specimen would be determined, and then statistical methods would be used to describe the represented population as a whole.

The fifth deliverable for this thesis will be three different predictions of the Young's and shear modulus of the material by using three different micromechanical models. The micromechanical models that will be used are:

- 1) The Eshelby model
- 2) The Self-Consistent model
- 3) The Mori-Tanaka model

The sixth deliverable for this thesis is an evaluation of how accurately the three different models were able to predict the Young's and shear modulus by comparing their predictions with the experimental results. A recommendation would be made on the ability of the current micromechanical models to predict the mechanical properties of the nanocomposite polymer.

As is common in research, unexpected results were found during tensile testing that prevented the research from being completed as planned. During tensile testing the nanocomposite polymer was found to behave in a manner that was unexpected for a homogeneous isotropic material. This change in behavior prevented the tensile testing from being completed as planned. A summary of the unexpected behavior, the changes in

methodology as a response to these findings, and a discussion of results as well as further research questions can be found in chapters 4, 5, and 6.

Chapter 2 – Literature Review

There are several different types of nanocomposite polymers; they can be classified by the type of geometry of the reinforcement. Some reinforcement geometries include: lamellar (platelet), fibrillar (small fibers), tubular, spherical as well as others. Different types of reinforcements provide different types of changes to the mechanical properties (Utracki, 2004).

A nanocomposite polymer consists of two main components, the polymeric material and a reinforcing material that has at least one dimension on the nano level (Koo, 2006). For ease of classification, there are three different requirements that can be met in order to have at least one dimension on the nano level. For fiber or tube fillers, the diameter must be less than 100 nm. For plate-like nanofillers, the thickness must be around the magnitude of 1 nm. For spherical or other equi-axed particles, the maximum dimension should be less than 100 nm (Ajayan, 2004).

The concentration of the reinforcement of a composite polymer is usually measured by the volume or weight fraction. The concentration of reinforcement is generally considered the single most important parameter that influences the characteristics of the composite polymer (Agarwal, 1990). Even though the concentration is considered the most important parameter, other factors can cause changes in the material properties.

Another important factor that can have an influence on the properties of a composite is the orientation of the reinforcement material. Since fibers have a 'long' dimension, they are not considered isotropic and will behave differently when loaded in

different directions. Fibers are generally used to carry load in the ‘long’ dimension; this creates a stronger polymer. In fibrous composites, the fiber is used to carry the load. At volume fractions of 0.2, the fiber is capable of carrying over 70% of the load (Mallick, 1993). Particles are considered to be spherical, they have no ‘long’ dimension and determining the orientation of the particles is neither feasible nor necessary (Agarwal, 1990). Since there are so many factors that can influence the mechanical characteristics of a polymer, it is useful to have ways to predict how these factors will interact with each other.

The mechanics of fiber reinforced composites are studied at two levels, the micromechanical level and the macromechanical level. The micromechanical level is concerned with the interaction of the constituent materials; especially the interaction between the constituents. The micromechanical level attempts to take into account the fact that the matrix will experience different stresses near the boundaries of the filler. The micromechanical level is contrasted by the macromechanical level which assumes that the material is homogeneous (Mallick, 1993).

There are several micromechanical models that can be used to predict the properties of an isotropic material that contains both reinforcements and voids. Of the several models that have been developed, three of them are of particular interest. These include: the Eshelby model, the Self-Consistent model, and the Mori-Tanaka model. Each of these models can be used to determine the Young’s modulus, E , and shear modulus, G , of the material (Park, 2005).

A possible material to use as reinforcement is a hexagonal platelet shaped kaolin clay particle. The geometry of the platelet has the equivalent circular diameter of 400–

6,000 nm and a thickness range of 4–600 nm. The ratio of the thickness to diameter is found to be 1/100-1/10. Although this geometry is clearly not symmetrical in all directions, there is an assumption that allows the platelet particles to be treated as spherical shapes. Previous research has shown that 3-D randomly oriented platelet particles can be treated as if they were spherical particles with an identical volume (Park, 2005).

Claims have been made that adding nano-sized clay particles as a reinforcement for a composite can offer improvements in various properties of the final composite. The addition of different nano-size reinforcement materials can result in improving a range of improvement of properties such as: flame retardation, increase in stiffness, increase in impact strength, and an increase in tensile strength. Information provided by the manufacturer of the composite material used for this thesis claims that the addition of the nano-size clay particles will increase mechanical strength of the final product. Since the method of fabrication of the test specimens for this thesis was injection molding, it is important to note that the manufacturer claims that the nano-size reinforcement particles will be well dispersed when the composite is used in extruders, mixers, and injection molders (Nanocor, 2006).

Although the three previously mentioned models (Eshelby, Self-Consistent, Mori-Tanaka) are designed to be used with spherical reinforcement particles, preliminary research has shown it may be possible to use these models for a composite that has hexagonal reinforcement particles. This can be done by using the platelet model; a model that is used to model randomly oriented hexagonal reinforcement particles as spheres (Park, 2005).

The platelet model begins by considering a composite in which the platelets are all oriented so that the ‘long’ directions of the particles are aligned with the x and y directions of the composite; this creates a transversely isotropic material. A stiffness matrix is then created to model the properties of the transversely isotropic material. The various components of the stiffness matrix are evaluated using properties of the resin, clay particles, and volume fractions of the resin, particles and voids (Park, 2007).

After the stiffness matrix for the transversely isotropic material has been established, it is necessary to modify the matrix so that it can represent a composite that has evenly distributed and randomly oriented clay particles. In order to accomplish this, the unidirectional model is rotated by an angle, θ , about the x-axis. This is done by using the 3-D transformation matrix $[T_x]$; this allows the transformed stiffness matrix to be computed. By integrating over a random value for θ , a new effective stiffness matrix, C' , is obtained. The transformed stiffness matrix is then rotated by an angle, ϕ , about the y-axis using the 3-D transformation matrix $[T_y]$. By integrating over a random value for ϕ , a new effective stiffness matrix, C'' , is obtained. It is not necessary to transform and integrate by the z-axis as the platelet particles are now evenly and randomly oriented about all three axes. The various components of the stiffness matrix can be calculated and used to evaluate the shear modulus as well as the extensional modulus of the composite material (Park, 2007).

In his research, Dr. Park has compared a platelet filler model with a spherical filler model. In this research, the material used for the experimental results contained platelet shaped clay reinforcement. The research found that the platelet model was consistently more accurate when compared to the experimental results, although the

maximum difference between the shear moduli calculated with the two models was 3.6% (Park, 2007). It is not surprising that the platelet model was more accurate at predicting the properties of a material with platelet reinforcement.

By including the use of the platelet model it is possible to use the three previously mentioned models, which require spherical reinforcement particles, to evaluate the bulk and shear modulus of a composite material which contains hexagonal reinforcement particles. Although each of the models takes a slightly different approach, they all use a modified version of Eshelby's tensor for spherical inclusions to model the reinforcement particles as spherical. The three models use properties of the resin and the clay particles as well as the volume fractions of the resin, reinforcement, and voids present. Several values for the Young's modulus and the shear modulus can then be calculated by using the three different models (Park, 2005).

Another factor that influences the properties of a polymer is the concentration distribution. If the concentration distribution is not uniform, weak points may be present in the part (Agarwal, 1990). This is because the enhanced characteristics from the reinforcement will be greater in some areas while weaker in others. It is important to have uniform distribution of the reinforcement material.

Another important factor that influences the properties of a composite is the size of the reinforcement material. Of particular interest is the concept that nano-sized particles can reinforce the matrix due to a better interface bondage with the matrix material (Park, 2007). Since the load is transferred from the matrix to the particles through the interface, using sub-micron particles can lead to significant improvement (Koo, 2006).

In addition to having an improved interfacial region, another advantage that nano-level reinforcements have over traditional sized reinforcements is that the amount of area that is classified as the interfacial region becomes a larger portion of the composite. This is true as long as the reinforcing nanoparticles are well dispersed and well distributed. Even if the interfacial region is only the space a few nanometers between the particles and the polymer, due to the large number of particles in any given volume a large portion of the polymer becomes part of the interfacial region (Ajayan, 2004).

One of the important interactions in any composite is the interaction between the polymer and the reinforcement; this is especially complicated in nanocomposites. The interaction between the polymer and the reinforcement material is important because it is where and how the load is transferred from the weaker polymer to the stiffer reinforcement. With composites that are on the nano level, the polymer chain and the reinforcement start to become similar in size. This allows the nano fillers to change the type or degree of the crystallinity which can influence the modulus of elasticity of the material. Part of the increase in strength seen in some nanocomposite polymers may be from the reinforcement restricting the movement of the polymer chains (Ajayan, 2004).

It is possible that part of the increase in the modulus of elasticity seen in some nanocomposite polymers may be due to the fact that adding equi-axed particles can alter the glass transition temperature, T_g , of the composite. This is important because the strength of a polymer is sensitive to the ambient temperature relative to the T_g of the composite. If the T_g of the polymer can be increased, the difference between the ambient temperature and the T_g can be increased. Therefore it is possible to increase the modulus of a composite by altering the T_g of the composite (Ajayan, 2004).

There are two theories that address the increase in modulus found in nanocomposites; although they are somewhat conflicting theories. One theory is the 'Bonded Polymer Theory'; this is the theory that there is more interfacial region for the same volume amount of reinforcement. This is due to the increased surface area per volume ratio for particles with a smaller radius. Research has shown that the 'Bonded Polymer Theory' is unable to explain the complete increase in the modulus of elasticity that has been found in nanocomposites. A second theory is the 'Double Network Theory', this address the idea that the interparticle distance starts to be comparable to the radius of gyration of the polymer chains. This allows the chains to form additional networks with the particles (Ajayan, 2004).

One of the primary advantages that nano-sized fillers have over conventional sized fillers is that the smaller size results in a smaller stress concentration factor. There can be a considerable amount of stress at the interaction between the matrix and the reinforcement. Larger particles sizes may cause cracks which are larger than the critical crack size; this can allow the crack to propagate and cause failure. With nano-level fillers, the crack size is likely to be smaller than the critical crack size which will prevent the crack from propagating and causing failure. This is what allows nanocomposites to gain the strength that traditional composites have without sacrificing ductility like normal composites experience (Ajayan, 2004).

An ideal composite material would only consist of the matrix material and the reinforcement material; however it is common for unwanted components to be present in composites. Fillers are often used to reduce costs without having a major effect on the final product. Additionally, voids are often present in composite materials. Since these

voids and fillers change the structure of the composite, there is a resulting change in material properties. It is recommended to take filler and voids into account when theoretically computing mechanical properties (Park, 2005).

In order to be able to do any sort of verification of these models, it is necessary to compare predictions of the models to actual data gathered from experiments. In order for an effective verification to be made, it is necessary that the experimental data is accurately measured. In the context of this thesis that includes the following information: force experienced during loading, cross sectional area of the test specimen, initial length of the test specimen, and change in length of the test specimen.

Since the test specimens have already been created prior to the start of this thesis, it is of particular interest to focus on the cross sectional area of the test specimen. Due to the fact that the existing set of test specimens have a concave shape which is visible to the naked eye, the cross sectional area cannot be reasonable or accurately measured using conventional methods such as a caliper or micrometer.

The geometry for the test specimens was chosen to adhere to the ASTM requirements for tensile testing of reinforced composites. It was decided to follow the ASTM because the ASTM has the standard test method to determine the tensile properties of reinforced plastics that are in the standard dumbbell shape (ASTM, 2003).

It is important to have an accurate measurement of the cross sectional area of the test specimen because the cross sectional area has a direct influence on the determined value of the Young's modulus. This can be seen in the following equation.

$$E = \frac{F * L_0}{A_0 * \Delta L} \quad (\text{Equation 1})$$

Where: $E = \text{Young's Modulus}$

$F = \text{Force Experienced}$

$L_0 = \text{Original Length of Test Specimen}$

$A_0 = \text{Original Cross Sectional Area of Test Specimen}$

$\Delta L = \text{Change in Length of Test Specimen}$

While the force, original length of the test specimen and change in length of the test specimen can all be measured using conventional methods, the cross sectional area of the current test specimens cannot be measured using conventional methods. Since this equation shows that any error in the measurement of the cross sectional area will result directly in error of the determined Young's modulus it is important that the cross sectional area of the test specimen is accurately obtained (Askeland, 1994).

An example calculation for all three models was done to generate a prediction for the Young's and shear modulus of a vinylester and kaolin clay nanocomposite polymer. Since each of the three models attempted to predict the final composite's materials using differing methods, the variation in final predictions is to be expected. A summary of the model's predictions can be seen in the Table 1.

Table 1: Young's and Shear Modulus Results from Models

Model	Young's Modulus	Shear Modulus
Eshelby	4.805 [GPa]	1.770 [GPa]
Mori-Tanaka	4.736 [GPa]	1.738 [GPa]
Self-Consistent	4.766 [GPa]	1.752 [GPa]
Mean	4.769 [GPa]	1.754 [GPa]
Standard Deviation of Population	0.028 [GPa]	0.013 [GPa]
Range	0.068 [GPa]	0.032 [GPa]

It is important to note that all three of these models generate similar results for the mechanical properties. This can be seen by looking at the standard deviation of the population for both the Young's and the shear modulus; with standard deviations of 0.028 GPa and 0.013 GPa respectively. The variations in predictions by the models are negligible from an engineering perspective where designs often include safety factors that are significantly greater than the 1.5% variation seen here. It is more significant to compare how the predictions from models compare to the experimental results.

In order to create a comparison between the experimental results and the theoretical models, all three of the theoretical models were used to predict the Young's and shear modulus of a sample nanocomposite polymer. The three models used were the Eshelby Model, the Mori-Tanaka Model, and the Self-Consistent Model. All three of the models used the same input parameters of the three base components of a sample composite. The vinyl ester resin was specified as 83.0% by volume, the kaolin clay was

specified as 15.7% by volume and total voids were specified as the remaining 1.3% by volume. The Young's modulus, shear modulus, and poisson's ratio for both the vinylester resin and kaolin clay were used while the voids were given no mechanical strength properties. Although the material properties of the vinylester resin are different than the nanocomposite used in this thesis, the same process can be applied to the nanocomposite polymer being studied for this thesis. The information for the vinylester resin nanocomposite is summarized in Table 2.

Table 2: Mechanical Properties of Components of a Sample Composite

Component	Percent by Volume	Young's Modulus	Shear Modulus	Poissons Ratio
Vinylester Resin	83.0 %	3.85 [GPa]	1.4 [GPa]	0.366
Kaolin Clay	15.7%	20 [GPa]	7.69 [GPa]	0.300
Total Voids	1.3%	N/A	N/A	N/A

Chapter 3 – Methodology

Before tensile testing of the specimens could begin, it was necessary to verify that the actual geometry of the parts are within the accepted variation allowed by the ASTM standard. The ASTM requires that reinforced composites shall follow the dimensions of their Type I specimen. This means that the dimensions for the test specimens were to be 6.50 inches long, 0.75 inches wide at the ends but narrows down to 0.50 inches wide in the middle, the narrow test area. The specimen will be approximately 0.25 inches thick across the entire specimen (ASTM, 2003). Unfortunately the existing test specimens have a concave shape along the length of the test specimen.

To some degree, these dimensions imply that the test specimen should have flat surfaces that fall within the tolerances of the specified dimensions. Although flatness is implied, there are no actual requirements that the test specimens have flat surfaces. The requirements are listed that the thickness of the test specimen shall be less than 0.28 inches [± 0.02 inches]. As long as all points on the surface of the test part fall within the 0.04 inch tolerance gap, as the specification is listed, it is not necessary that any two points have the same thickness (ASTM, 2003).

In order to verify that the test specimens have a geometry that adheres to the ASTM, the actual dimensions of the test specimens needed to be accurately measured. A caliper was used to measure the width and the length of the test specimens. Due to the unexpected concave shape of the top and bottom surfaces of the specimens, the thickness could not be adequately measured using a caliper. Since a caliper could not be used, a different measurement process was applied.

The measurement of the thickness of the test specimens was done by creating a process that used a coordinate measuring machine. The coordinate measuring machine was used because it had a measuring tip that could fit within the shallowest section of the test surface, was able to consistently measure multiple test specimens, and was able to measure accurately within 0.01 inches as required by the ASTM. The process included a method to secure the test specimen during measurements, the number and location of measurements made, the program code that ran the coordinate measuring machine, and a method to record the data produced by the program.

It was important to physically secure the test specimens during testing because any movement of the specimen during measuring would result in an error of the measurement of the dimensions. In addition to preventing an individual test specimen from moving, it was beneficial to secure all test specimens in the same location inside the coordinate measuring machine's working surface so that a single program could be used for all of the test specimens. The parts were secured by a Kurt AngLock D675 vise. The clamp was secured to the coordinate measuring machines surface using two bolts that were secured directly into the working surface; this made sure that the clamp would not move during or in between any of the measuring cycles. Each test specimen was held in place while the clamp was tightened. In each case, the clamp was tightened enough to prevent the specimen from moving, but not enough to deform the test specimen itself.

In order to get an accurate measurement of the surface of the test specimens, measurements were taken along the narrow test portion of the specimens. The narrow test portion of the specimens is 2.00 inches long and 0.50 inches wide. Measurements were taken every 0.25 inches along this testing area, which resulted in 9 'lines' to be measured

on both the top and the bottom of the test specimen. At each of these lines, the coordinates were measured at the peak height on one side of the test specimen ($A_{Top, n}$) then the coordinates at the middle of the test portion was measured ($B_{Top, n}$) and finally the peak height on the other side of the test specimen was taken ($C_{Top, n}$). After each set of three points was measured, the process was repeated 0.25 inches further down the test specimen ($A_{Top, n+1}$, $B_{Top, n+1}$, $C_{Top, n+1}$). This resulted in 27 data points for each side of each test specimen. Since the surfaces were concave on both sides of the test specimen, the specimen was then “rotated” 180° along its long axis and the process was repeated on the other side. This resulted in 9 profiles along the narrow length of the test specimen. Each profile contained 6 data points, 3 on the top and 3 on the bottom side ($A_{Top, n}$; $B_{Top, n}$; $C_{Top, n}$; $A_{Bottom, n}$; $B_{Bottom, n}$; $C_{Bottom, n}$)

The program code written to measure the thickness of the test specimen was written following guidelines in the Brown & Sharpe Micro-Hite DCC’s reference manual (Wilcox, 2005). A summary of the procedure of the code is as follows; see Appendix A for the complete code. After the test specimen was secured in the clamp, the operator manually established the top plane of the test specimen by contacting the probe at three points along the surface of the test specimen. The points were taken at the same location for all specimens, two points at the end of the test strip on one side and one point in the middle of the test strip on the other side. Establishing the location of the top plane of the specimen defined the reference point for the Z, or vertical, coordinates (Wilcox, 2005).

Next, the operator manually established the side of the test specimen by contacting the probe at two points along the side of the test strip area. The points were taken in the same order and at the same location for all test specimens. The left point was

taken towards the end of the test portion of the test specimen followed by the right point which was taken towards the other end of the test portion of the test specimen. This established the reference location and direction for the X coordinates. By using this procedure, it would not have been necessary to load the test specimen in the same spot in the clamp every time; however, the test specimens were loaded at the very edge of the clamp every time to avoid any unexpected confounding factors that may have occurred (Wilcox, 2005).

Finally, the operator manually established the location of the clamp by contacting the probe at two points along the left most face of the clamp. In a similar method to the previous points taken along the test specimen, these points were taken in the same order and at the same location for all test specimens. The first point was taken along the clamps surface closest to the operator followed by the second point which was taken along the clamps surface further away from the operator. This established the reference location and direction for the Y coordinates (Wilcox, 2005).

Following this procedure before measuring the surface of any test specimens established a consistent and custom coordinate system for each test surface. By defining a plane and two lines, a custom origin was selected 0.75 inches above the intersection of the plane and the intersection of the two lines. The variable that was controlled in this procedure was that the test specimen had to be loaded the 'long' way in the clamp. This was able to be done by lining up the flat sides on each end of the test specimen with the flat surfaces of the clamp. Since the program was able to start at the same location relative to the test specimen, the rest of the program was able to be executed in automatic mode; the operator did not need to manually control the probe. The program then

measured the coordinates of each of the 27 points described earlier and then the data was collected and stored. After the first side was done, the specimen was turned over and the process was repeated for the other side.

The data from the measuring process was used to determine the actual cross sectional area of the test specimen. The ASTM dictated that the width and thickness of the cross sectional area be measure at each end of the narrow test section and that those two numbers would be average to give the cross sectional area used in calculations. The procedure of this research deviated from the recommended process by measuring the cross sectional area at 9 points along the narrow test area and then averaging the data. Before taking shrinkage into account the cross sectional area of the test specimen was calculated to be 0.13 square inches. Since the data from the coordinate measuring machine provided 2 peak heights and 1 valley height, the cross sectional area was calculated assuming a straight line connection between the peaks and the valley. This resulted in an oversized, which results in a conservative, estimate of the cross sectional area of the test specimen. The conservative cross sectional area was found to be 0.12 square inches; this is a 7.7% reduction in area due to shrinkage.

In addition to determining the cross sectional area of the test specimen, the collected data was able to verify that the test specimens met the requirements for thickness. The thickness for the specimens was found to average 0.263 inches. The range in variation of thickness along the length of an individual test specimen was found to average 0.007 inches with a maximum of 0.009 inches. This was found to be within the requirements listed in the ASTM standard which state that that the thickness of the test specimen shall be less than 0.28 inches [± 0.02 inches].

The mechanical testing consisted of a tensile test to determine the tensile properties of the nanocomposite material; ten specimens were to be tested. The tensile test would have been conducted according to the procedure laid out in the ASTM. The procedure is very comprehensive; it includes the settings to be used for the tensile test machine, desired ambient conditions during testing, as well as conditioning of the specimens for at least 40 hours prior to testing. If equipment limitations require any deviations from the guidelines in the ASTM, they will be documented.

The ASTM dictates that a minimum number of 5 specimens need to be tested in order for the data obtained by this test method to be relevant and appropriate for use in engineering design. There were 25 specimens that were determined to be quality specimens for tensile testing that were created using the injection molding procedure followed by Stuart Boyd in *Application of Injection Molding for the Purpose of Testing Nanoclay-Reinforced Composite Polypropylene*. Out of these 25 specimens, 10 contiguous samples from the fabrication process were selected to be used for tensile testing; this exceeded the requirements stated by the ASTM. The remaining 15 specimens were used during a pilot test to verify that the following test procedure was set up properly.

The mechanical testing of the specimens followed the ASTM guidelines that are applicable for the tensile testing of a reinforced composite that has the standard dumbbell shape. In order to measure the strain of the test specimen, an extensometer was attached directly onto the specimen. The extensometer selected was a MTS 634.25E-2X Axial Extensometer which had an initial span of 2.00 inches. The 2.00 inch span of the extensometer was placed over the 2.00 inch narrow testing portion of the test specimen.

The speed setting for the machine was selected to follow ASTM. For Type I specimens, the speed of testing was 0.20 inch/minute. These settings were selected so that the test specimen would rupture in approximately 30 seconds to 5 minutes of testing. The clamps of the tensile testing machine were set as per the ASTM which says that the clamps were to be set at the lowest pressure that prevents slipping of the test specimen and without crushing the test specimen.

During testing of the specimen, both load and strain were measured simultaneously. The load was measured from the MTS 810 Material Test System tensile testing machine and strain was measured with the previously mentioned extensometer which was attached directly to the specimen. This procedure allowed all the necessary information required to calculate the Young's modulus of the composite polymer (ASTM, 2003).

Chapter 4 – Findings from Tensile Testing

As is a common occurrence when conducting research, unexpected results were found during initial tensile testing. A recurring problem was found when attempting to verify that the tensile testing machine was setup properly. While using excess test specimens to verify that the tensile testing procedure and data collection was set up properly, it was found that all test specimens were breaking in the same relative location which was outside of the narrow testing area. This was unexpected because the breaks were occurring where the test specimen was relatively thick when compared to the narrow testing area. This was unexpected for a homogeneous material because failure is expected to occur at the area where the stress is the highest. Since stress is a function of force over area and the entire test sample is receiving the same load, the section with the smallest cross sectional area should be the point of failure (Shackelford, 2000). All 4 specimens broke in the wide area on the opposite side of where the gate was located during the fabrication process; this can be seen in Figure 1.



Figure 1: First Four Specimens after Tensile Test

The unexpected failure mode of the composite was problematic to the continuation of this research. On page 6 of the ASTM, it says to “discard specimens that break at some flaw, or that break outside of the narrow cross-sectional test section”. The material was found to behave in a way that prevents the research from following the ASTM. Additionally, the behavior of the material acted in a way that was not compatible with the assumption made by the three models that the material is a homogenous isotropic material. Therefore, additional research into the behavior of the test specimens was conducted.

Chapter 5 – Revised Methodology and Results

Since the material was not exhibiting the behavior expected for a homogeneous material, some test specimens were examined further using explorative methods. Another specimen was loaded “flipped” 180° to be loaded “upside down” when compared to previously test specimens. This was done to see if the consistent location of the failures was being caused by the tensile testing machine itself; however, it was found that orientation of the specimen had no effect. All specimens broke at the wide area on the end opposite the gate. The recurring failure outside of the narrow test section for all 5 test specimens can be seen in Figure 2. The extra failure on the two rightmost specimens was caused by further testing which is described later in this thesis.



Figure 2: All Five Specimens after Tensile Test

As an explorative measure, two of the previously tested specimens were re-tested in the tensile testing machine. The test was conducted using the previously defined methodology with the only variation being that due to previous testing the test specimens were shorter. After the load was applied to these test specimens, the failure point was found to be at the same end that the first failure had occurred; as seen in Figure 3.



Figure 3: Specimens That Were Tested Twice

Since the first sign of abnormal behavior was consistently occurring at the end of the test specimen that was furthest away from the gate, both ends of a test specimen were cut off. The ends were cut perpendicular to the long axis of the test specimen. After examining the internal faces that were exposed, initial results showed that there appears to be a cone-shaped core that forms inside of the test specimen with the thickest cross section being located at the end furthest away from the gate. This is shown as a difference

in coloration and lines that seem to indicate that a boundary has formed on the inside of the test specimen. This can be seen in Figure 4.



Figure 4: Specimen with Ends Cut Off

In an effort to further investigate the unexpected behavior of the material, an impact test was conducted on a test specimen. The impact test was done using a Terco MT3016 Impact Tester. The shear value for the impact test was recorded as 2.15 joules. After the impact test, the test specimen broke into three distinct pieces. After looking at the exposed surfaces, it was seen that the core of the test specimen is visible in the narrow cross sectional testing area. This indicates that the material is not homogenous in the narrow cross sectional area as seen in Figure 5.



Figure 5: Specimen after Impact Test

In order to examine the location along the entire long axis of the test specimens, another test specimen was cut into 8 segments. These cuts were made in the same perpendicular fashion as the cuts in the previous test specimen. It was found that the core exists almost along the entire length of the test specimen. The core also appears to gradually grow in size as it gets further away from the gate end of the test specimen. Since the diameter of the core section varies along the length of the test specimen, it indicates that the core is not present in the same magnitude throughout the entire specimen; this can be seen in Figure 6.

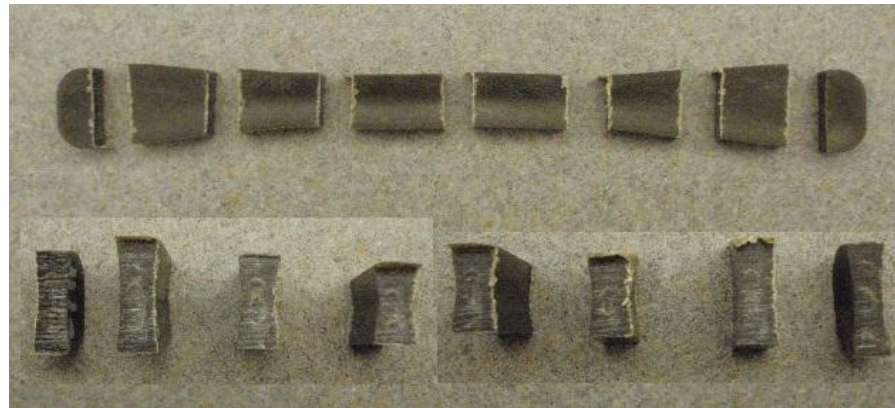


Figure 6: Specimen that was cut into Slices

The next explorative cut was done by creating a diagonal cut that passed through the wide end of each side of the specimen. On the end of the test specimen that is closest to the gate, the cut went smoothly and no problems occurred. When the exposed surfaces were examined, at least 11 vertical lines could be seen spread throughout the width of the test specimen. This indicates that the material is not forming into a single homogenous part, but that layers do appear to form during fabrication. This can be seen in Figure 7.



Figure 7: Specimen with end cut at Diagonal

When the same diagonal cut was attempted on the side of the test specimen that is furthest away from the gate, the cut was going smoothly until the blade hit what appeared to be the core inside the specimen. The core section of the test specimen behaved as a material with greater strength as it resisted the cut and was rapidly pulled out of clamp when the teeth of the saw blade sunk into the core. Although only some of the outside material was removed by this cut, the remains partially exposed the core. The partially exposed core can be seen in Figure 8.



Figure 8: Partial Core Exposed After Attempting Diagonal Cut

When examining the broken test specimens, it was found that there appears to be a core inside of the test specimens. Even though the core is made out of the same material, it appears to behave differently than the outer portions of the test specimens.

In order to verify that the core is more than just an appearance issue and does actually have different material properties, a hardness test was conducted. A New Age Industries HP-DR durometer was used. The durometer used for the testing used the Type D scale for hardened plastics. A test specimen was cut on the opposite end of the gate perpendicular to its long axis; this created a flat surface that was ideal for hardness testing. The hardness was measured at two locations: first outside of the core and secondly inside of the core. The hardness of the outer material was found to be 54 while the core material was found to be 68. Although the hardness scale is unitless, the higher value recorded for the core material indicates it is a harder material (Schaffer, 1999).

Chapter 6 – Conclusion and Future Research

The data from the preliminary tensile testing was analyzed to show an initial comparison between the experimental data and the three predictions that were created by the models. It was found that the Young's modulus for the test specimen was 388,000 psi; this is the equivalent of 2.67 GPa. The Young's modulus can be seen in Figure 9 which is the Stress-Strain graph of one of the test specimens that was used in a tensile test.

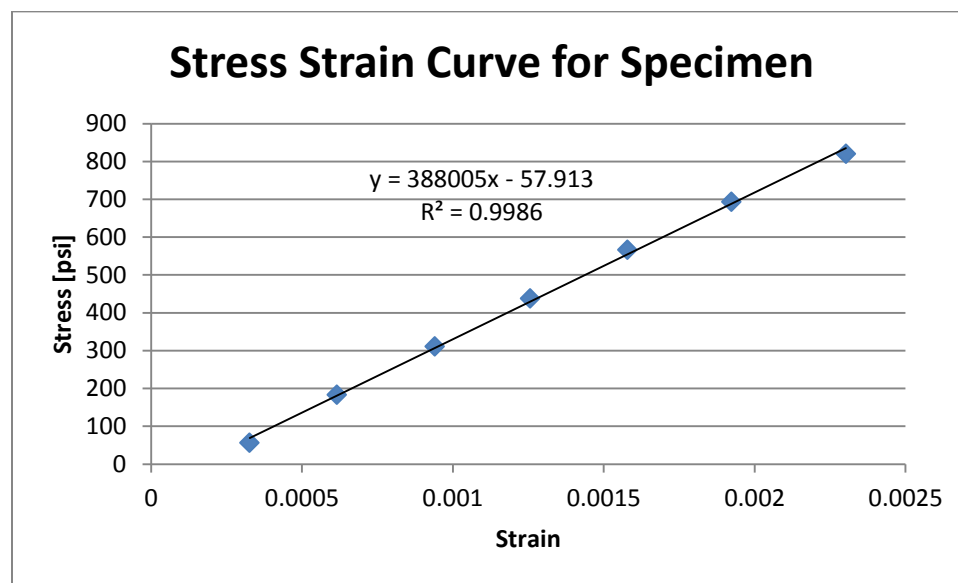


Figure 9: Stress Strain Curve of a Test Specimen after Tensile Test

However, the value of 2.67 GPa for the Young's modulus should not be used for comparison with predictions made by the three models. Since the failures during tensile testing occurred outside of the area where strain data was collected, necessary information for calculating the Young's and shear modulus is unavailable. Without

having accurate strain data for the location of the failure, calculating the Young's and shear modulus would be meaningless. Without the Young's and shear modulus of the test specimens, it is unnecessary to use the three models to predict the Young's and shear modulus of the nanocomposite used in this thesis.

There were two primary types of models that were to be considered for predicting the mechanical properties of this nanocomposite material; the spherical model and the platelet model. The platelet model derives its equations by considering a hypothetical composite where all of the reinforcement particles are platelet shaped and are all aligned so that the long dimensions are all along the x-axis. The hypothetical composite is then rotated randomly about the x and then y-axis to model a composite that has randomly oriented reinforcing particles (Park, 2007). This creates a model that assumes the material is isotropic and homogeneous. This model predicts that the test specimen would break where the stress is the highest; in this case, where the cross sectional area is the smallest. This assumption is incompatible with the behavior that the material exhibited during testing.

The spherical model derives its equations by using the Eshelby model and its variations, Mori-Tanaka and Self-Consistent models, to determine the properties of the nanocomposite. These models use the volume fractions of the resin, filler, and voids as well as the mechanical properties of the individual components to determine the strength of the materials as a composite material (Park, 2005). As with the platelet model, the spherical model works off of the assumption that the material is homogeneous and therefore has isotropic characteristics.

Since the behavior of the material during tensile testing is exhibiting characteristics that violate the assumptions made by the three different models, it is not reasonable to compare experimental results with the theoretical predictions.

There are several future research questions that should be answered in order to continue the preliminary research found in this thesis. The main question that needs to be answered is that of why does the core form in the test specimens. There are several experiments and areas of research that may provide insight into the formation of this core, this includes:

- Investigate cooling of specimen during injection molding process
- Use a heated mold during injection molding process
- Investigate dispersion of nanoparticles
- Investigate failure surfaces using an appropriate microscope

It would be beneficial to investigate the cooling of the specimen that occurs during the injection molding process. It is possible that the test specimen does not cool at the same rate throughout the entire specimen. If the specimens were not cooling uniformly during the injection molding process, it could possibly explain the formation of layers that were seen during exploratory testing. Investigation into using a heated mold to control uniform cooling of the test specimen may yield answers.

An experiment should be conducted in which variables such as the injection temperature of the composite, the mold temperature, and rate of cooling are controlled and varied. The specimens should then be examined to determine whether or not fabrication variables have an influence on the formation of the core. If a core is found to

appear, hardness tests should be conducted on both the core and outer material. By documenting any possible relationship between fabrication variables and core properties further insight may be gained into the formation, behavior and significance of the core.

Another way to investigate the unexpected behavior found in the test specimens would be to investigate if the nanoparticles are actually well dispersed throughout the test specimens. Although the manufacturer claims that injection molding would result in well dispersed particles, it is possible that orientation and displacement of the particles was influenced during the injection molding process. This investigation could be done using high-powered microscopes or other appropriate observation techniques.

Since all the failures occurred in close proximity to the clamps of the tensile testing machine, future research should be done to investigate any relationship between the clamping forces and the location of failure. The hypothesis that the failure location is due to forces from the clamps of the testing machine has a low probability of being correct. When specimens were loaded upside down, the failure still occurred in the same relative location on the test specimen, regardless of which set of clamps were acting on the test specimen. Although the probability of this hypothesis being correct is low, it should be investigated in an effort to document and/or reduce confounding factors.

Reference List

- (Agarwal, 1990) Agarwal, Bhagwan D., et al., *Analysis and Performance of Fiber Composites*, 2nd ed., John Wiley & Sons, Inc. (1990).
- (Ajayan, 2004) Ajayan, Pulickel, M., et al., *Nanocomposite Science and Technology*, 2004, Wiley-VCH, Weinheim, Germany.
- (Askeland, 1994) Askeland, Donald R., *The Science and Engineering of Materials*, PWS Publishing Company, Boston, MA (1994).
- (ASTM, 2003) ASTM D 638, *Standard Test Method for Tensile Properties of Plastics*, American Society for Testing and Materials, Philadelphia (2003).
- (Barbero, 2011) Barbero, Ever J., *Introduction to Composite Materials Design*, 2nd ed., 2011, Boca Raton, Florida.
- (Boyd, 2011) Boyd, Stuart., *Application of Injection Molding for the Purpose of Testing Nanoclay-Reinforced Composite Polypropylene*, Minnesota State University, Mankato, MN (2011).
- (Koo, 2006) Koo, Joseph H., *Polymer Nanocomposites – Processing, Characterization, and Applications*, McGraw-Hill, New York (2006).
- (Mallick, 1993) Mallick, P. K., *Fiber-Reinforced Composites*, 2nd ed., Marcel Dekker, New York (1993).
- (Nanocor, 2006) Nanocor, Inc., *NanoMax Masterbatch Products Technical Data*, http://www.nanocor.com/tech_sheets/P802.pdf <March, 20120>, Hoffman Estates, IL (2006).
- (Park, 2005) Park, Jin Y., et al., *Effect of Filler and Void Content on Mechanical Properties of Pultruded Composite Materials Under Shear Loading*, Journal of Polymer Composites, (2005).
- (Park, 2007) Park, Jin Y., et al., *Shape Effect of Platelet Clay Filler on Mechanical Behaviors of Pultruded Polymer Composites under Shear Loading*, Journal of Reinforced Plastics and Composites, Vol. 26, No. 6, Sage Publications (2007).

- (Schafer, 1999) Schaffer, James P., et al. *The Science and Design of Engineering Materials*, McGraw-Hill, Boston, MA (1999).
- (Shackelford, 2000) Shackelford, James F., *Materials Science for Engineers*, Prentice Hall, New Jersey (2000).
- (Utracki, 2004) Utracki, Leszek A., *Clay-Containing Polymeric Nanocomposites*, 2004, Rapra Technology Limited, UK.
- (Wilcox, 2005) Wilcox Associates, Inc., *PC-DMIS 4.1 Reference Manual* (2005).
- (Wilson, 2002) Wilson, Mick, et al., *Nanotechnology – Basic Science and Emerging Technologies*, 2002, Chapman & Hall/CRC, University of New South Wales Press Ltd., Sydney, Australia.

Appendix A – CMM Code and Data Collection for a Test Specimen

ART NAME : Tensile Test Specimen

REV NUMBER : 1

SER NUMBER : Test Subject

STATS COUNT : 1

STARTUP =ALIGNMENT/START,RECALL:,LIST=YES

ALIGNMENT/END

MODE/MANUAL

CHECK/ 0.1,1

MOVESPEED/ 30

TOUCHSPEED/ 0.7

MANRETRACT/5

FORMAT/TEXT,OPTIONS,ID,HEADINGS, , ;MEAS,NOM,TOL,DEV,OUTTOL, ,

LOADPROBE/B89

TIP/T1A0B0, SHANKIJK=0, 0, 1, ANGLE=0

\$\$ NO,Define 1 plane, 2 lines, and a point to so computer can locate the part

PLN1 - TOP OF SPECIMEN=FEAT/PLANE,CARTESIAN,TRIANGLE

THEO/<8.83834,0.40699,-15.56512>,<-0.0036883,0.0022557,0.9999907>

ACTL/<8.8048,0.40655,-15.56352>,<0.004323,-0.0017561,0.9999891>

MEAS/PLANE,3

HIT/BASIC,NORMAL,<8.36492,0.2405,-15.56649>,<-
0.0036874,0.0022569,0.9999907>,<8.41379,0.24896,-15.56211>,USE THEO = YES

HIT/BASIC,NORMAL,<9.34976,0.24042,-15.56286>,<-
0.0036874,0.0022569,0.9999907>,<9.27354,0.24899,-15.56583>,USE THEO = YES

HIT/BASIC,NORMAL,<8.79991,0.74033,-15.56601>,<-
0.0036874,0.0022569,0.9999907>,<8.72707,0.7217,-15.56263>,USE THEO = YES

ENDMEAS/

LIN1 - ALONG TEST AREA=FEAT/LINE,CARTESIAN,UNBOUNDED

THEO/<8.53018,0.23917,-15.64077>,<0.9999988,0.0015697,0>

ACTL/<8.46036,0.23351,-15.61784>,<0.9999825,0.0059163,0>

MEAS/LINE,2,WORKPLANE

HIT/BASIC,NORMAL,<8.53021,0.23917,-15.64078>,<0.0015697,-0.9999988,0>,<8.46036,0.23351,-15.61819>,USE THEO = YES

HIT/BASIC,NORMAL,<9.40248,0.24054,-15.64079>,<0.0015697,-0.9999988,0>,<9.24067,0.23813,-15.61749>,USE THEO = YES

ENDMEAS/

LIN2 - ALONG CLAMP, FIXED SIDE=FEAT/LINE,CARTESIAN,UNBOUNDED

THEO/<5.7952,0.39181,-14.21668>,<-0.0023034,0.9999973,0>

ACTL/<5.79502,0.74609,-14.17845>,<-0.002409,0.9999971,0>

MEAS/LINE,2,WORKPLANE

HIT/BASIC,NORMAL,<5.7952,0.39204,-14.21665>,<0.9999973,0.0023034,0>,<5.79502,0.74609,-14.17848>,USE THEO = YES

HIT/BASIC,NORMAL,<5.79313,1.29243,-14.21671>,<0.9999973,0.0023034,0>,<5.79345,1.39728,-14.17842>,USE THEO = YES

ENDMEAS/

PNT2 - INTERSECTION OF LINE 1, 2=FEAT/POINT,CARTESIAN,NO

THEO/<5.79557,0.23488,-14.92873>,<0.9999988,0.0015697,0>

ACTL/<5.7963,0.21775,-14.89814>,<0.9999825,0.0059163,0>

CONSTR/POINT,INT,LIN1 - ALONG TEST AREA,LIN2 - ALONG CLAMP, FIXED SIDE

MODE/DCC

\$\$ NO,Start alignment to set up XYZ origin location

A1 =ALIGNMENT/START,RECALL:STARTUP,LIST=YES

ALIGNMENT/LEVEL,ZPLUS,PLN1 - TOP OF SPECIMEN

ALIGNMENT/ROTATE,XPLUS,TO,LIN1 - ALONG TEST AREA,ABOUT,ZPLUS

ALIGNMENT/TRANS,XAXIS,PNT2 - INTERSECTION OF LINE 1, 2

```

ALIGNMENT/TRANS,YAXIS,PNT2 - INTERSECTION OF LINE 1, 2
ALIGNMENT/TRANS,ZAXIS,PNT2 - INTERSECTION OF LINE 1, 2
ALIGNMENT/END
$$ NO,Define the clear plane, 2.75 inches above z plane/top of part
$$ NO,Move probe to starting position
    CLEARP/ZPLUS,2.75,ZPLUS,0,OFF
$$ NO,Move probe to a starting position
    MOVE/POINT,NORMAL,<2.25,0,-0.25>
$$ NO, *****Start Collecting Line 0 Data*****
PNT2 - LINE 0,A=FEAT/POINT,CARTESIAN
    THEO/<2.24868,0.00079,-0.64767>,<0,0,1>
    ACTL/<2.24848,0.00097,-0.65265>,<0,0,1>
    MEAS/POINT,1
    HIT/BASIC,NORMAL,<2.24868,0.00079,-0.64767>,<0,0,1>,<2.24848,0.00097,-
0.65265>,USE THEO = YES
    ENDMEAS/
    MOVE/POINT,NORMAL,<2.25,0.25,-0.25>
PNT3 - LINE 0,B=FEAT/POINT,CARTESIAN
    THEO/<2.24859,0.25087,-0.67303>,<0,0,1>
    ACTL/<2.24851,0.25074,-0.68323>,<0,0,1>
    MEAS/POINT,1
    HIT/BASIC,NORMAL,<2.24859,0.25087,-0.67303>,<0,0,1>,<2.24851,0.25074,-
0.68323>,USE THEO = YES
    ENDMEAS/
    MOVE/POINT,NORMAL,<2.25,0.5,-0.25>
PNT4 - LINE 0,C=FEAT/POINT,CARTESIAN
    THEO/<2.24867,0.50082,-0.6469>,<0,0,1>

```

ACTL/<2.24865,0.50069,-0.65399>,<0,0,1>

MEAS/POINT,1

HIT/BASIC,NORMAL,<2.24867,0.50082,-0.6469>,<0,0,1>,<2.24865,0.50069,-0.65399>,USE
THEO = YES

ENDMEAS/

\$\$ NO,*****Stop Collecting Line 0*****

\$\$ NO,*****Start Collecting Line 1*****

MOVE/POINT,NORMAL,<2.5,0,-0.25>

PNT26 LINE 1,A=FEAT/POINT,CARTESIAN

THEO/<2.49875,0.00086,-0.64743>,<0,0,1>

ACTL/<2.49838,0.00103,-0.65193>,<0,0,1>

MEAS/POINT,1

HIT/BASIC,NORMAL,<2.49875,0.00086,-0.64743>,<0,0,1>,<2.49838,0.00103,-
0.65193>,USE THEO = YES

ENDMEAS/

MOVE/POINT,NORMAL,<2.5,0.25,-0.25>

PNT27 LINE 1,B=FEAT/POINT,CARTESIAN

THEO/<2.49856,0.25047,-0.67673>,<0,0,1>

ACTL/<2.49824,0.25036,-0.68394>,<0,0,1>

MEAS/POINT,1

HIT/BASIC,NORMAL,<2.49856,0.25047,-0.67673>,<0,0,1>,<2.49824,0.25036,-
0.68394>,USE THEO = YES

ENDMEAS/

MOVE/POINT,NORMAL,<2.5,0.5,-0.25>

PNT28 LINE 1,C=FEAT/POINT,CARTESIAN

THEO/<2.49868,0.50082,-0.6472>,<0,0,1>

ACTL/<2.49841,0.50066,-0.65448>,<0,0,1>

MEAS/POINT,1

HIT/BASIC,NORMAL,<2.49868,0.50082,-0.6472>,<0,0,1>,<2.49841,0.50066,-0.65448>,USE
THEO = YES

ENDMEAS/

\$\$ NO,*****Stop Collecting Line 1*****

\$\$ NO,*****Start Collecting Line 2*****

MOVE/POINT,NORMAL,<2.75,0,-0.25>

PNT5 LINE 2,A=FEAT/POINT,CARTESIAN

THEO/<2.74867,0.00078,-0.64756>,<0,0,1>

ACTL/<2.74842,0.00094,-0.65229>,<0,0,1>

MEAS/POINT,1

HIT/BASIC,NORMAL,<2.74867,0.00078,-0.64756>,<0,0,1>,<2.74842,0.00094,-
0.65229>,USE THEO = YES

ENDMEAS/

MOVE/POINT,NORMAL,<2.75,0.25,-0.25>

PNT6 LINE 2,B=FEAT/POINT,CARTESIAN

THEO/<2.74861,0.25078,-0.67761>,<0,0,1>

ACTL/<2.74843,0.25066,-0.68413>,<0,0,1>

MEAS/POINT,1

HIT/BASIC,NORMAL,<2.74861,0.25078,-0.67761>,<0,0,1>,<2.74843,0.25066,-
0.68413>,USE THEO = YES

ENDMEAS/

MOVE/POINT,NORMAL,<2.75,0.5,-0.25>

PNT7 LINE 2,C=FEAT/POINT,CARTESIAN

THEO/<2.7487,0.50082,-0.64712>,<0,0,1>

ACTL/<2.74856,0.50065,-0.65493>,<0,0,1>

MEAS/POINT,1

HIT/BASIC,NORMAL,<2.7487,0.50082,-0.64712>,<0,0,1>,<2.74856,0.50065,-0.65493>,USE
THEO = YES

```

ENDMEAS/
$$ NO,*****Stop Collecting Line 2*****
$$ NO,*****Start Collecting Line 3*****
MOVE/POINT,NORMAL,<3,0,-0.25>
PNT8 LINE 3,A=FEAT/POINT,CARTESIAN
THEO/<2.9986,0.00094,-0.64741>,<0,0,1>
ACTL/<2.99823,0.00107,-0.65266>,<0,0,1>
MEAS/POINT,1
HIT/BASIC,NORMAL,<2.9986,0.00094,-0.64741>,<0,0,1>,<2.99823,0.00107,-0.65266>,USE
THEO = YES
ENDMEAS/
MOVE/POINT,NORMAL,<3,0.25,-0.25>
PNT9 LINE 3,B=FEAT/POINT,CARTESIAN
THEO/<2.99863,0.25064,-0.67844>,<0,0,1>
ACTL/<2.99832,0.25051,-0.68336>,<0,0,1>
MEAS/POINT,1
HIT/BASIC,NORMAL,<2.99863,0.25064,-0.67844>,<0,0,1>,<2.99832,0.25051,-
0.68336>,USE THEO = YES
ENDMEAS/
MOVE/POINT,NORMAL,<3,0.5,-0.25>
PNT10 LINE 3,C=FEAT/POINT,CARTESIAN
THEO/<2.99868,0.50082,-0.64707>,<0,0,1>
ACTL/<2.99841,0.50066,-0.65472>,<0,0,1>
MEAS/POINT,1
HIT/BASIC,NORMAL,<2.99868,0.50082,-0.64707>,<0,0,1>,<2.99841,0.50066,-
0.65472>,USE THEO = YES
ENDMEAS/
$$ NO,*****Stop Collecting Line 3*****

```

\$\$ NO,*****Start Collecting Line 4*****

MOVE/POINT,NORMAL,<3.25,0,-0.25>

PNT11 LINE 4,A=FEAT/POINT,CARTESIAN

THEO/<3.24865,0.00081,-0.64744>,<0,0,1>

ACTL/<3.24824,0.00096,-0.65323>,<0,0,1>

MEAS/POINT,1

HIT/BASIC,NORMAL,<3.24865,0.00081,-0.64744>,<0,0,1>,<3.24824,0.00096,-0.65323>,USE THEO = YES

ENDMEAS/

MOVE/POINT,NORMAL,<3.25,0.25,-0.25>

PNT12 LINE 4,B=FEAT/POINT,CARTESIAN

THEO/<3.2486,0.25084,-0.67824>,<0,0,1>

ACTL/<3.24824,0.2507,-0.68315>,<0,0,1>

MEAS/POINT,1

HIT/BASIC,NORMAL,<3.2486,0.25084,-0.67824>,<0,0,1>,<3.24824,0.2507,-0.68315>,USE THEO = YES

ENDMEAS/

MOVE/POINT,NORMAL,<3.25,0.5,-0.25>

PNT13 LINE 4,C=FEAT/POINT,CARTESIAN

THEO/<3.24868,0.5008,-0.64635>,<0,0,1>

ACTL/<3.24834,0.50065,-0.6547>,<0,0,1>

MEAS/POINT,1

HIT/BASIC,NORMAL,<3.24868,0.5008,-0.64635>,<0,0,1>,<3.24834,0.50065,-0.6547>,USE THEO = YES

ENDMEAS/

\$\$ NO,*****Stop Collecting Line 4*****

\$\$ NO,*****Start Collecting Line 5*****

MOVE/POINT,NORMAL,<3.5,0,-0.25>

PNT14 LINE 5,A=FEAT/POINT,CARTESIAN

THEO/<3.49867,0.00079,-0.64714>,<0,0,1>

ACTL/<3.4982,0.00099,-0.65276>,<0,0,1>

MEAS/POINT,1

HIT/BASIC,NORMAL,<3.49867,0.00079,-0.64714>,<0,0,1>,<3.4982,0.00099,-0.65276>,USE
THEO = YES

ENDMEAS/

MOVE/POINT,NORMAL,<3.5,0.25,-0.25>

PNT15 LINE 5,B=FEAT/POINT,CARTESIAN

THEO/<3.49861,0.25081,-0.67764>,<0,0,1>

ACTL/<3.49825,0.25065,-0.68283>,<0,0,1>

MEAS/POINT,1

HIT/BASIC,NORMAL,<3.49861,0.25081,-0.67764>,<0,0,1>,<3.49825,0.25065,-
0.68283>,USE THEO = YES

ENDMEAS/

MOVE/POINT,NORMAL,<3.5,0.5,-0.25>

PNT16 LINE 5,C=FEAT/POINT,CARTESIAN

THEO/<3.4987,0.50081,-0.64672>,<0,0,1>

ACTL/<3.4984,0.50066,-0.65413>,<0,0,1>

MEAS/POINT,1

HIT/BASIC,NORMAL,<3.4987,0.50081,-0.64672>,<0,0,1>,<3.4984,0.50066,-0.65413>,USE
THEO = YES

ENDMEAS/

\$\$ NO,*****Stop Collecting Line 5*****

\$\$ NO,*****Start Collecting Line 6*****

MOVE/POINT,NORMAL,<3.75,0,-0.25>

PNT17 LINE 6,A=FEAT/POINT,CARTESIAN

THEO/<3.74871,0.00081,-0.64734>,<0,0,1>

```

ACTL/<3.74838,0.00101,-0.65298>,<0,0,1>
MEAS/POINT,1
HIT/BASIC,NORMAL,<3.74871,0.00081,-0.64734>,<0,0,1>,<3.74838,0.00101,-
0.65298>,USE THEO = YES
ENDMEAS/
MOVE/POINT,NORMAL,<3.75,0.25,-0.25>
PNT18 LINE 6,B=FEAT/POINT,CARTESIAN
THEO/<3.74868,0.2504,-0.67837>,<0,0,1>
ACTL/<3.7484,0.25024,-0.68304>,<0,0,1>
MEAS/POINT,1
HIT/BASIC,NORMAL,<3.74868,0.2504,-0.67837>,<0,0,1>,<3.7484,0.25024,-0.68304>,USE
THEO = YES
ENDMEAS/
MOVE/POINT,NORMAL,<3.75,0.5,-0.25>
PNT19 LINE 6,C=FEAT/POINT,CARTESIAN
THEO/<3.74873,0.50081,-0.64642>,<0,0,1>
ACTL/<3.74848,0.50065,-0.65505>,<0,0,1>
MEAS/POINT,1
HIT/BASIC,NORMAL,<3.74873,0.50081,-0.64642>,<0,0,1>,<3.74848,0.50065,-
0.65505>,USE THEO = YES
ENDMEAS/
$$ NO,*****Stop Collecting Line 6*****
$$ NO,*****Start Collecting Line 7*****
MOVE/POINT,NORMAL,<4,0,-0.25>
PNT20 LINE 7,A=FEAT/POINT,CARTESIAN
THEO/<3.99868,0.0008,-0.64648>,<0,0,1>
ACTL/<3.9983,0.00096,-0.6529>,<0,0,1>
MEAS/POINT,1

```

HIT/BASIC,NORMAL,<3.99868,0.0008,-0.64648>,<0,0,1>,<3.9983,0.00096,-0.6529>,USE
THEO = YES

ENDMEAS/

MOVE/POINT,NORMAL,<4,0.25,-0.25>

PNT21 LINE 7,B=FEAT/POINT,CARTESIAN

THEO/<3.99858,0.25083,-0.67774>,<0,0,1>

ACTL/<3.99831,0.25069,-0.68222>,<0,0,1>

MEAS/POINT,1

HIT/BASIC,NORMAL,<3.99858,0.25083,-0.67774>,<0,0,1>,<3.99831,0.25069,-
0.68222>,USE THEO = YES

ENDMEAS/

MOVE/POINT,NORMAL,<4,0.5,-0.25>

PNT22 LINE 7,C=FEAT/POINT,CARTESIAN

THEO/<3.99868,0.50079,-0.6463>,<0,0,1>

ACTL/<3.99846,0.50064,-0.65472>,<0,0,1>

MEAS/POINT,1

HIT/BASIC,NORMAL,<3.99868,0.50079,-0.6463>,<0,0,1>,<3.99846,0.50064,-0.65472>,USE
THEO = YES

ENDMEAS/

\$\$ NO,*****Stop Collecting Line 7*****

\$\$ NO,*****Start Collecting Line 8*****

MOVE/POINT,NORMAL,<4.25,0,-0.25>

PNT23 LINE 8,A=FEAT/POINT,CARTESIAN

THEO/<4.24869,0.00077,-0.64633>,<0,0,1>

ACTL/<4.24823,0.00093,-0.65283>,<0,0,1>

MEAS/POINT,1

HIT/BASIC,NORMAL,<4.24869,0.00077,-0.64633>,<0,0,1>,<4.24823,0.00093,-
0.65283>,USE THEO = YES

```

ENDMEAS/
MOVE/POINT,NORMAL,<4.25,0.25,-0.25>
PNT24 LINE 8,B=FEAT/POINT,CARTESIAN
THEO/<4.24859,0.25085,-0.67524>,<0,0,1>
ACTL/<4.24822,0.25076,-0.68066>,<0,0,1>
MEAS/POINT,1
HIT/BASIC,NORMAL,<4.24859,0.25085,-0.67524>,<0,0,1>,<4.24822,0.25076,-
0.68066>,USE THEO = YES
ENDMEAS/
MOVE/POINT,NORMAL,<4.25,0.5,-0.25>
PNT25 LINE 8,C=FEAT/POINT,CARTESIAN
THEO/<4.24869,0.50081,-0.6457>,<0,0,1>
ACTL/<4.24834,0.50063,-0.65395>,<0,0,1>
MEAS/POINT,1
HIT/BASIC,NORMAL,<4.24869,0.50081,-0.6457>,<0,0,1>,<4.24834,0.50063,-0.65395>,USE
THEO = YES
ENDMEAS/
$$ NO,*****Stop Collecting Line 8*****
$$ NO,*****Start Collecting Line 9*****
MOVE/POINT,NORMAL,<4.5,0,-0.25>
CS1   =REPORT/CUSTOM, FILENAME= custom report name, AUTOPRINT=NO, Section=-1
PARAM/=
ENDCUSTOM/

```

